ELSEVIER

Journal of Chromatography B, 737 (2000) 25–38

JOURNAL OF CHROMATOGRAPHY B

www.elsevier.com/locate/chromb

Preparative two-step purification of recombinant human basic fibroblast growth factor from high-cell-density cultivation of *Eschericia coli*

Gunnar Garke, Wolf-Dieter Deckwer, Friedrich Birger Anspach*

Biochemical Engineering Division, GBF-Gesellschaft für Biotechnologische Forschung mbH, Mascheroder Weg 1, D-38124 Braunschweig, Germany

Abstract

Aggregation and precipitation are major pitfalls during bioprocessing and purification of recombinant human basic fibroblast growth factor (rh-bFGF). In order to gain high yields of the soluble protein monomer with high biological activity, an efficient downstream process was developed, focussing on the combination of expanded bed adsorption (EBA) and heparin chromatography. After expression in *E. coli* TG1:pλFGFB, cells were harvested and washed; then the rh-bFGF was released via high pressure homogenization. The high viscosity of the feedstock of about 40 mPa s, showing non-newtonian behaviour, was reduced to 2 mPa s by the addition of DNase. The homogenate (5.6 l) was loaded directly on an expanded bed column (C-50) packed with the strong cation-exchanger Streamline™ SP. In the eluates, histone-like (HU) protein was identified as the main protein contaminant by sequence analysis. The thermodynamics and kinetics of rh-bFGF adsorption from the whole broth protein mixture were determined in view of competition and displacement effects with host-derived proteins. Optimal binding and elution conditions were developed with knowledge of the dependence of rh-bFGF adsorption isotherms on the salt concentration to allow direct application of eluates onto Heparin HyperD™. This affinity support maintained selectivity and efficiency under CIP and over a wide range of flow-rates; both is advantageous for the flexibility of the purification protocol in view of a scalable process. Remaining DNA and HU protein were separated by Heparin HyperD. The endotoxin level decreased from ≈1,000,000 EU/ml in the whole broth to 10 EU in 3 mg bFGF per ml. The final purification protocol yields >99% pure rh-bFGF as judged from SDS-PAGE and MALDI–TOF mass spectrometry with high mitogenic activity (ED_{50}=1–1.5 ng/ml) of the lyophilized sample. In comparison to the conventional process, the overall protein recovery rose by 15% to 65% with saving time and costs.

Keywords: Purification; *Escherichia coli*; Recombinant human basic fibroblast growth factor

1. Introduction

Human basic fibroblast growth factor (h-bFGF) is a single-chain, non glycosylated protein. It contains 154 amino acids, has a molar mass of $17.3 \cdot 10^3$ and modulates both cell proliferation and cell differentiation in vitro and in vivo [1,2]. BFGF can be isolated from many different tissue extracts, e.g. brain and pituitary, with the restriction of low concentrations in these sources (between 10^{-9} and 10^{-11} *M*). To make available greater amounts of h-bFGF, it was produced in recombinant *E. coli* [3,4]. As a mitogen, h-bFGF is a potent mediator for wound healing, angiogenesis and tissue regeneration [5,6]. Its po-

*Corresponding author. Tel.: +49-531-6181-743; fax: +49-531-6181-175.
E-mail address: Anspach@gbf.de (F.B. Anspach)

0378-4347/00/$ – see front matter
PII: S0378-4347(99)00394-1

tential for clinical use is currently evaluated for the treatment of stroke, peripheral vascular disease and coronary artery disease in phases II and III [7].

For purification the strong interaction of h-bFGF with glycosaminoglycans, such as heparin and heparan sulfate, is widely utilized. Although the mechanism has not been solved yet, in vivo, this interaction plays an important role for receptor binding and signal transduction [5]. The highly negative charged heparin is a group-selective ligand, which interacts more or less specifically with many proteins. Thus, obtaining homogeneous protein preparations in a single step is not possible. Heparin affinity chromatography is commonly combined with a cation-exchange step, maybe followed from subsequent purification steps, such as copper chelate or hydrophobic interaction or gel permeation chromatography [8–10].

On a larger scale the removal of cell debris and cells is a general problem as clogging of the chromatographic equipment must be prevented. Usually, small-scale centrifugal separation assures up to 99.99% reduction of cell content and 90% product recovery. However, the centrifugation of larger volumes results in poorer separation, so that additional microfiltration is necessary. Although not in the special case of high-cell-density cultivation, but in most other microbial processes, the reduction of process volumes is important at the beginning of a downstream process. Ultrafiltration, besides adsorption, precipitation and partitioning is a well-proven technique for this purpose, but it is limited by membrane fouling. To combine clarification, capture and concentration in one step, the expanded bed technique was introduced for the purification of protein-containing feedstocks (for reviews see [11–13]). The expanded bed is a special form of a solid–liquid fluidized bed, where particles of a size ratio >2.2 are used. The broad size distribution causes a classification of the particles during fluidization with little mixing, which causes homogeneous flow through the bed. Besides investigations with model systems, indicating the good performance of this technique with single proteins [14,15], several applications from distinct sources like yeasts [16,17], bacterial cells [18,19] and cell cultures [20,21] can be found. Expanded bed adsorption was found an easy technique to scale up, with column diameters up to 600 mm to be employed [22]. Besides the reduction of the number of purification steps, fast removal of proteolytic enzymes and a shortening of the total process time may help to prevent losses in mass and quality of recombinant h-bFGF (rh-bFGF) due to degradation and precipitation.

In adsorption chromatography with particulate matrices, high protein binding capacities are bound to a porous structure and a high accessible inner surface area of sorbents. However, then the flow-rate is limited owing to mass transport resistances in the pores of the chromatographic particles. At higher flow-rates and also with scaling up a process, compression may be observed for common soft gels in the packed bed. To overcome these problems, macroporous particles were developed showing less diffusion restriction [23]. Also a gel-in-shell particle [24] was introduced that combines the stability of a rigid skeleton with the high capacity of traditional soft gels.

In the following investigation a two-step purification scheme for soluble rh-bFGF from a high cell density cultivation of *E. coli* is introduced. The expanded bed cation-exchange adsorber Streamline™ SP is employed as well as the affinity chromatographic sorbent Heparin HyperD™, which is based on a gel-in-shell particle. Special attention was paid on the development of a timesaving purification protocol that requires a minimum of steps.

2. Theoretical considerations

According to Stokes' law, the bed expansion in a column depends, among other parameters, on the viscosity of the applied solution. As the viscosity of microbial homogenates is higher than water and strongly varies with the composition and concentration of the biomass, it cannot be predicted but must be measured. This is usually done by plotting the shear stress against the shear rate by using a rheometer, yielding the viscosity which is to be expected under operating conditions. Only if newtonian behaviour applies or the solution is very diluted, the viscosity can be directly obtained from the slope of this graph. Furthermore, only then the simple dependence of the shear rate, $\dot{\gamma}$, from the linear

liquid velocity, u_0, and the particle diameter, d_p, according to Eq. (1) is valid.

$$\dot{\gamma} = \frac{u_0}{d_p} \tag{1}$$

However, at high concentrations of a biopolymer solution, non newtonian behaviour of the fluid is a common observation. This has the consequence that the viscosity is shear rate dependent. A better approximation of the shear rate in an expanded bed column is provided by Eq. (2), considering the flow index, m, and the voidage of the expanded bed, ε [25]. The flow index can be obtained from the power law (3), with τ, the fluid shear stress and K, the consistency index to be obtained from viscosity measurements at different shear rates. From the flow index the shear rate to be considered during expanded bed adsorption can be estimated. As the shear rate in the expanded bed is very low (<10 s^{-1}), the viscosity is to be extrapolated from the tangential slope of the power law graph at very low shear rates.

$$\dot{\gamma} = \frac{12u_0(1-\varepsilon)}{\varepsilon^2 d_p} \times \frac{3m+1}{4m} \tag{2}$$

$$\tau = K\dot{\gamma}^m \tag{3}$$

The voidage of the expanded bed depends on the degree of bed expansion, which is the ratio, h/h_0, of expanded and settled bed heights. According to Richardson and Zaki [26], Eq. (4) correlates u_0 and the terminal settling velocity u_t of a particle with ε and the expansion index, n.

$$\frac{u_0}{u_t} = \varepsilon^n \tag{4}$$

They also showed that n depends only on the terminal Reynolds number, Re_t, of a particle. For $Re_t < 0.2$, $n = 4.65$ is constant. It should be mentioned, that the values of n depend both on the particle and fluid properties. Furthermore, the most fundamental investigations on fluidization were performed with particles of uniform spheres, high densities and greater particle diameters as used in ion-exchange chromatography. Besides d_p, the viscosity, η, and g, the gravitational acceleration, u_t depends on the densities of adsorbent, ρ_p, and liquid, ρ_l, and can be estimated from the Stokes' law (Eq. 5). A more comprehensive description of the hydrodynamics in liquid fluidization is provided by di Felici [27].

$$u_t = \frac{(\rho_p - \rho_l)d_p^2 g}{18\eta} \tag{5}$$

Assuming the volume of the solid-phase does not change with bed expansion, h/h_0 can be calculated from Eq. (6) with a porosity of the settled bed, ε_0, of 0.42, as obtained from Eqs. (4) and (5).

$$\frac{h}{h_0} = \frac{(1-\varepsilon_0)}{(1-\varepsilon)} \tag{6}$$

3. Experimental

3.1. Materials

Ethylenediaminetetraacetic acid disodium salt dihydrate (EDTA) was obtained from Fluka (Buchs, Switzerland) and DNase I from Boehringer Mannheim (Mannheim, Germany). Streamline™ SP was purchased from Pharmacia Biotech (Uppsala, Sweden) and Heparin HyperD from BioSepra (Villeneuve la Garenne, Cedex, France). Other chemicals and salts were purchased from E. Merck (Darmstadt, Germany) in analytical grade.

3.2. Instrumentation and columns

For expanded bed adsorption a C-50 column (Pharmacia Biotech, Uppsala, Sweden) with a column diameter of 5 cm was used. All liquids were pumped with two Ismatec MV-Z gear pumps (Zürich, Switzerland). Flow rates were measured with two magnetic flow sensors MG 711/F4 (Turbo-Werk Messtechnik, Cologne, Germany) and controlled by a computer. The absorbance was detected with a UV/VIS photometer Knauer 732.97 (Knauer, Berlin, Germany). Conductivity and pH were measured with a digital conductometer type 600 and a pH meter 762, respectively, from Knick (Berlin, Germany). Data acquisition and system control, including a digital I/O board CIO-DDA06 (Computer Boards, Mansfield, MA, USA) and an analog I/O board DAS-8PGA (Keithley Metrabyte, Taunton, MA, USA), were guided with the computer

programme DAMOCLeS written in HTBasic (Trans-Era, Provo, UT, USA), running on a personal computer. The eluates were collected with a Supra-Frac (Pharmacia Biotech, Uppsala, Sweden).

Heparin affinity chromatography was carried out on an FPLC system including two P-500 pumps, a controller LCC-500 Plus, a fraction collector Frac-100 (Pharmacia Biotech, Uppsala, Sweden) and a UV detector (280 nm) UV 2510 UVICORD SD (LKB, Bromma, Sweden). The Heparin HyperD sorbent was packed into a HR 10/10 column (Pharmacia Biotech, Uppsala, Sweden) with 1 cm diameter.

3.3. Methods

3.3.1. Production of rh-bFGF

Rh-bFGF was produced in high cell density cultivation of *E. coli* TG1:pλFGFB [28]. Although about 25% of total rh-bFGF formed as inclusion bodies during cultivation, this insoluble protein fraction was ignored. 25 l were harvested by pumping the cell suspension into 150 l washing buffer of 100 m*M* sodium phosphate (NaPi) buffer, containing 150 m*M* NaCl and 10 m*M* EDTA (pH 7.0). The aim was to remove medium components and contaminants from the fermentation medium like antifoaming agents. After stirring for 15 min the cells were separated at 9200 rpm at 10 l/h with an intermittent desludging of the disk stack separator CSA8 (Westfalia Separator AG, Oelde, Germany) and resuspended in 20 l of 50 m*M* NaPi buffer (pH 7.0). Soluble rh-bFGF was released from the periplasma by single passage through a high-pressure homogenizer SHL05 (Bran+Luebbe GmbH, Norderstedt, Germany) at 900 bar and 1 l/min. No special focus was spent at the optimization of the product release from *E. coli* cells. In order to keep the viscosity low, 600 mg DNase was added to the cell suspension before cell disruption. After this treatment, 1 m*M* EDTA was added and 3.5 l of the cell homogenate was applied after further dilution directly to the expanded bed column, the remaining solution was stored at −20°C for further investigations.

3.3.2. Expanded bed adsorption

For expanded bed adsorption the C-50 column (diameter of 5 cm) was filled with 304 ml of the strong cation-exchanger Streamline SP, yielding a sedimented bed height of 15.5 cm. Before loading, the bed was equilibrated with 10 column volumes of buffer A, containing 50 m*M* NaPi+40 m*M* NaCl+1 m*M* EDTA (pH 7.0, $\kappa = 10.0$ mS/cm), at a volumetric flow-rate of 2945 ml/h, corresponding to a superficial velocity of 150 cm/h. With a measured bed height of 26.6 cm ($h/h_0 = 1.7$) the upper adapter was set to 44 cm. 3.5 l of the crude cell homogenate was adjusted from pH 6.62 to 7.00 with 6 *M* NaOH and from $\kappa = 9.9$ mS/cm to $\kappa = 10.0$ mS/cm with solid NaCl. Afterwards the feedstock was diluted with buffer to 5.58 l to reduce the viscosity further (bio wet mass 11.5%, bio dry weight 2.5%). After loading and washing, the flow was reversed and the adapter lowered to the upper boundary of the column bed. Elution was done in the packed bed mode with reversed flow at a volumetric flow-rate of 1180 ml/h (superficial velocity 60 cm/h) within 10 column volumes (CV), corresponding to 3040 ml buffer B with 50 m*M* NaPi+1.2 *M* NaCl+1 m*M* EDTA (pH 7.0, $\kappa = 102.7$ mS/cm).

3.3.3. Heparin affinity chromatography

Before loading, the Heparin HyperD column (10.8×1 cm, 8.5 ml column volume) was washed with 10 CV with the equilibration buffer consisting of 50 m*M* NaPi+0.5 *M* NaCl+1 m*M* EDTA (pH 6.3) at flow-rates indicated in the figure legends. After loading up to 540 ml of the sample and washing with 3 CV, linear gradient elution was performed with 3 *M* NaCl in the equilibration buffer within 26 CV.

3.3.4. Rh-bFGF quantification

For the quantification of rh-bFGF in the homogenate an analytical chromatographic procedure was developed as described [29]. Briefly, after centrifuging the crude feedstocks for 30 min at 40 000 *g*, the supernatants were applied onto a UNO-S1 column (BIORAD, Munich, Germany). For the calibration, purified rh-bFGF was injected from dialysed fractions of heparin eluates, whose protein content was determined by the Lowry method [30].

3.3.5. Electrophoresis

SDS–PAGE was done in a Multiphor II unit with a power supply EPS 3500 XL and using precast

ExcelGel®SDS gradient gels (8–18% and 12–14%) and buffer strips, all from Pharmacia Biotech (Uppsala, Sweden). Sample treatment under reducing conditions and staining with Coomassie blue G 250 were carried out as recommended by the supplier, according to [31].

3.3.6. Viscosity measurements

The viscosity of the various solutions was determined using a rotational coaxial cylinder rheometer Rheomat O/115 (Contraves, Zürich, Switzerland) with variable speed at 25°C. Shear rates were chosen between 0.5 and 900 s^{-1} and allowing 10 s for equilibration before reading the shear stress.

3.3.7. Bioassay

Mitogenic activity of rh-bFGF was determined by incorporation of ^{3}H-thymidine into the DNA of serum-depleted BALB 3T3 cells, as described [32]. Each concentration was measured three times in parallel.

3.3.8. Endotoxin assay

The endotoxin content was determined using a quantitative, chromogenic *Limulus* amoebocyte lysate (LAL) assay (endpoint method) following the instructions of the supplier (Chromogenix, Sweden).

4. Results and discussion

4.1. Properties of the feedstream

Rh-bFGF is produced in recombinant *E. coli* as an intracellular protein processed into the periplasma. About 75% of soluble protein is obtained under the chosen cultivation conditions with the remaining being accumulated as inclusion bodies. Product release is achieved either by bead mill cell disruption or by high pressure homogenization, which typically results in feedstock properties as shown in Table 1. Although sonification yields a better deterioration of DNA, leading to a better fluidity of the feedstreams, this method is not practicable on larger scales. The major problems with the other two methods are the highly viscous feedstreams. To allow for a better handling and processing, the large DNA chains were cut in smaller fragments by the restriction enzyme DNase I. The enzyme was added before homogenization, as the viscosity is lowered immediately after cell disruption [33]. Furthermore, the enzyme activity is higher owing to an increase of the temperature during homogenization. Therefore, the process time is shortened before loading the homogenate onto the expanded bed column.

Table 1
Feed properties of *E. coli* homogenate

Whole cells and cell debris
High protein concentration
High viscosity owing to the DNA content
Protease activity
High endotoxin concentration
low ionic strength

After cell disruption the pH was 6.62 and the conductivity 9.9 mS/cm. Bio wet mass was determined to 18.3%, corresponding to 4.0% bio dry mass. The dependence of the shear stress on increasing shear rates was studied with and without addition of DNase at two bio mass contents (Fig. 1). The experimental curves could be well-described by the power law (see Eq. (3)) with the parameters shown in Table 2. Using Eq. (1), the shear rate relevant in expanded bed adsorption is estimated to 2.1 s^{-1} at the linear flow-rate of 150 cm/h employed here. In contrast, with Eq. (2) shear rates are calculated between 9 and 10 s^{-1}, depending on the properties of the feedstream. Fitting shear rates linearly in the

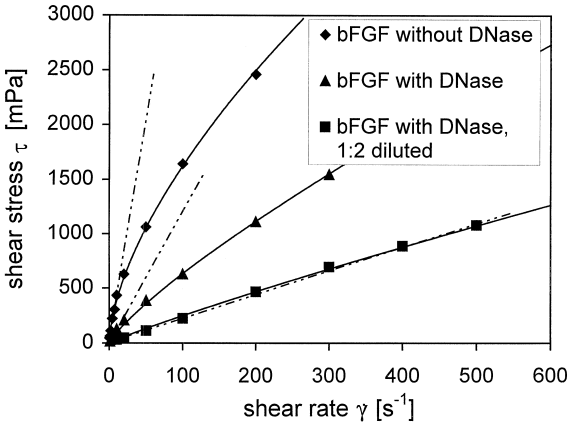

Fig. 1. Rheogram of *E. coli* homogenates before and after DNase treatment and at different bio mass content. Curves were fitted linearly at low shear rates and employing the power law (for parameters see Table 2).

Table 2
Power law (Ostwald) parameters of rheograms from Fig. 1

	Bio wet mass	Consistancy index K (mPa)	flow index m	linear slope or viscosity (mPa s)
Without DNase	19.3%	91.38	0.624	40
With DNase	21.3%	14.56	0.818	12
With DNase, 1:2 diluted	10.7%	3.83	0.906	2.2

lower shear regions with the tangential slopes representing the viscosity results in the data summarized in Table 2. The DNase drastically lowers the viscosity of the crude feedstock from 40 to 12 mPa s. Dilution further reduces the viscosity to about 2 mPa s, which is acceptable to work with in expanded bed adsorption, resulting only in mediate further expansion to $h/h_0 = 2.6$. At 12 mPa s this expansion is more dramatic, causing built-up of particles at the upper column adapter. Without the addition of DNase the expanded bed collapsed, causing the fluid flow to partially bypass the particle bed.

Fig. 2 displays experimental data and curve shapes as calculated according to Eqs. (4) and (5) of the bed expansion in dependence of flow-rate and viscosity. Experimental data are obtained from glycerol solutions with viscosities as indicated. For the calculations an expansion index of $n = 5$ was applied. The bed expansion with the crude *E. coli* homogenate at 150 cm/h is also indicated and is found in good agreement with the theory. It is to be considered that these calculations are based on assumptions and simplifications, but it makes clear that the viscosity is a very important factor for a given chromatographic setup, especially when handling biomass feedstocks. Data from literature are rare regarding biomass content, viscosity and degree of bed expansion with *E. coli* homogenates. Barnfield Frej et al. [33] recommend a biomass dry mass of 3.5% and a viscosity of less than 10 mPa s at a shear rate of 1 s^{-1}. It was mentioned that also feedstocks with a viscosity of 50 mPa s at 1 s^{-1} can be handled. Johansson et al. [19] applied a feedstock with 0.6% dry cell mass without commenting upon the viscosity. However, it is mentioned that the bed collapsed at concentrations below 50 m*M* Tris. It is difficult to compare these data and to outline general limits for operation regimes.

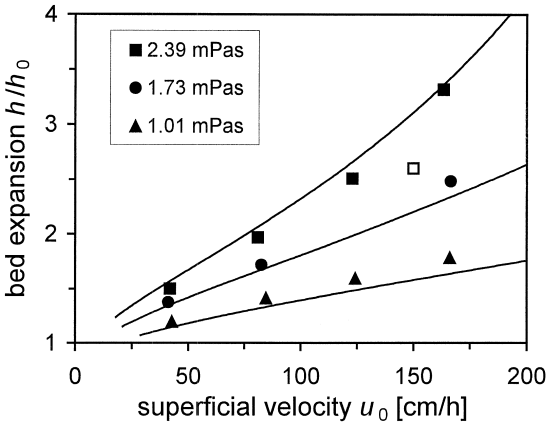

Fig. 2. Relative bed heights in expanded bed adsorption with Streamline SP at different viscosities of liquids. ■ = 29.3% (w/w), ● = 20.0% (w/w), ▲ = 0% glycerol in 20 m*M* NaPi buffer. Solid lines were calculated with Eqs. (4) and (5). The experimentally derived expansion with *E. coli* homogenate is included (□).

From Eq. (5) it is deduced to chose an adsorber matrix with high particle density in order to compensate for a high viscosity and thus to allow fast processing. An increase of the particle diameter would be even more effective to achieve a higher terminal settling velocity. However, the latter causes additional mass transfer restrictions for a product to diffuse through the film and into the particle, leading to a decrease of the dynamic binding capacity.

Besides this, also the dependence of viscosity on the degree of cell disruption must be considered, causing low reproducibilities of feedstocks from the same bio mass source. Moreover, the determination of the viscosity from particle-containing samples may cause problems due to bad mixing or sedimentation of solids. In the case of non newtonian

behaviour of the fluid the shear rate should also be mentioned for comparison of the bed expansion. Using feedstocks from different microorganisms as well as different types of ion-exchangers and changing pHs or conductivities, many other parameters come into play influencing the stability of the expanded bed.

4.2. Thermodynamics and kinetics of rh-bFGF adsorption

To get knowledge about the protein binding capacity of the expanded bed column, batch equilibrium and uptake experiments were performed with the crude homogenate. Fig. 3 shows adsorption isotherms of rh-bFGF on Streamline SP at two distinct ionic strengths. The Langmuir-shape isotherm originates from a relatively high NaCl concentration of 40 m*M* in the buffer, corresponding to 10 mS/cm. Usually, 2–3 mS/cm are recommended to support binding on ion-exchange sorbents. Yet, a high capacity of 65 mg/ml rh-bFGF was found. Product binding under such conditions is favourable for an ion-exchange process, as most host-derived proteins do not bind or bind only in low amounts. At 150 m*M* NaCl the capacity decreases noticeably and so the binding conditions for expanded bed adsorption were adjusted to 10 mS/cm.

The range of data points at both ionic strengths displays the typical problems when utilizing the batch mode to study adsorption isotherms with real protein mixtures. If the protein concentration is low at the beginning, getting information about a wide concentration range is not possible. However, also at high protein concentrations the equilibrium concentration will never get equal to the original rh-bFGF concentration of the feedstock, which is, however, important for process development. The only way to manage this in batch mode is to increase the rh-bFGF concentration in the feedstock by adding pure rh-bFGF before adsorption. This has the disadvantage that the ratio of target to host-derived proteins is changed, which, on the other hand also happens during normal adsorption. Each single equilibrium point shown in Fig. 3 displays a different composition of the liquid phase that is distinct from the original feedstock. If competition comes into play this may cause a lower dynamic binding capacity in the column mode as expected from batch adsorption isotherms.

Another point to consider is the influence of the viscosity on the rate of protein uptake, which affects the breakthrough behaviour respectively the dynamic binding capacity of the column. Fig. 4 displays rh-bFGF uptake from whole broth, including fitting of the experimental data to a film and pore diffusion

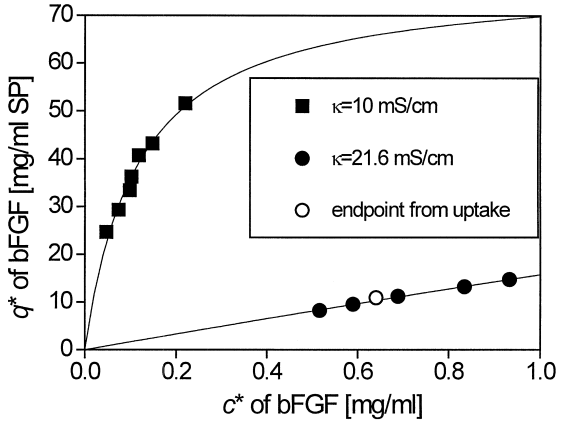

Fig. 3. Batch adsorption isotherms of rh-bFGF from crude *E. coli* homogenate on Streamline SP in 50 m*M* NaPi+40 m*M* NaCl+1 m*M* EDTA, pH 7, $\kappa = 10$ mS/cm and 50 m*M* NaPi+0.15 *M* NaCl+1 m*M* EDTA, pH 7, $\kappa = 21.6$ mS/cm. The data were fitted (solid lines) with the Langmuir equation and $q_m = 77.9$ mg/ml, $K_D = 0.116$ mg/ml (■) and $q_m = 250$ mg/ml, $K_D = 14.87$ mg/ml (●).

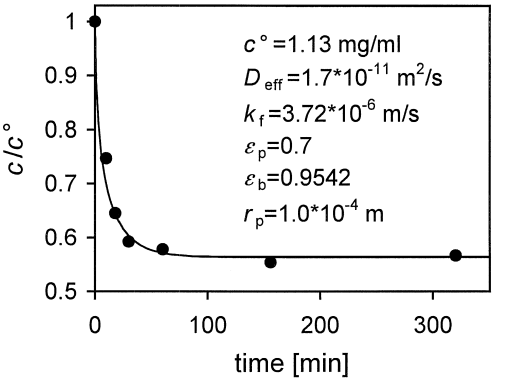

Fig. 4. Batch adsorption uptake of rh-bFGF from crude *E. coli* homogenate on Streamline SP in 50 m*M* NaPi+0.15 *M* NaCl+1 m*M* EDTA, pH 7, $\kappa = 21.6$ mS/cm. The solid line was calculated with the film and pore diffusion model.

model [34]. The heterogeneous particle model based on the differential mass balance equation was solved numerically. It was used earlier to describe the uptake of model proteins on Streamline SP [35]. The effective pore diffusion coefficient, D_{eff}, for rh-bFGF is lower than the free diffusivity ($D_0 = 9.0 \cdot 10^{-11}$ m^2/s), as calculated according to Young et al. [36]. However, in view of the high viscosity and the inhomogeneity of the whole broth the difference is similar on fixed bed sorbents and using normal protein solutions. Furthermore, no indication of a reaction rate limitation between rh-bFGF and the surface of Streamline SP was found. Overall these results indicate that the intraparticle mass transport is not determined by additional limitations that would otherwise prevent a good performance in the expanded bed mode.

4.3. Expanded bed adsorption

The experimental setup was checked applying a tracer (1% v/v acetone in buffer) as negative step input signal (data not shown). This allows to discover a nonuniform flow distribution in the column or instabilities of the expanded bed. This procedure yielded a number of theoretical plates, $N = 47$, which is in good agreement with other reports [22]. Mentioning that this value only characterises the column setup is important, as it does not guarantee a good separation. In the presence of biomass feedstock, the fluidization changes and flow inhomogeneities may develop, causing a decrease of *N*. In this context it would be interesting to investigate the change in *N* with addition of whole broth and using NaCl as a tracer.

After loading the feedstock (see Section 4.1) and washing, bound proteins eluted from the packed bed with NaCl at ionic strengths from 25 to 50 mS/cm (Fig. 5). SDS–PAGE gels revealed rh-bFGF as the main constituent in elution fractions. Another protein coeluted at the same salt concentration which was identified as histone-like (HU) protein from N-terminal sequence analysis. This is a DNA-binding protein with an isoelectric point between 9.6 and 9.7

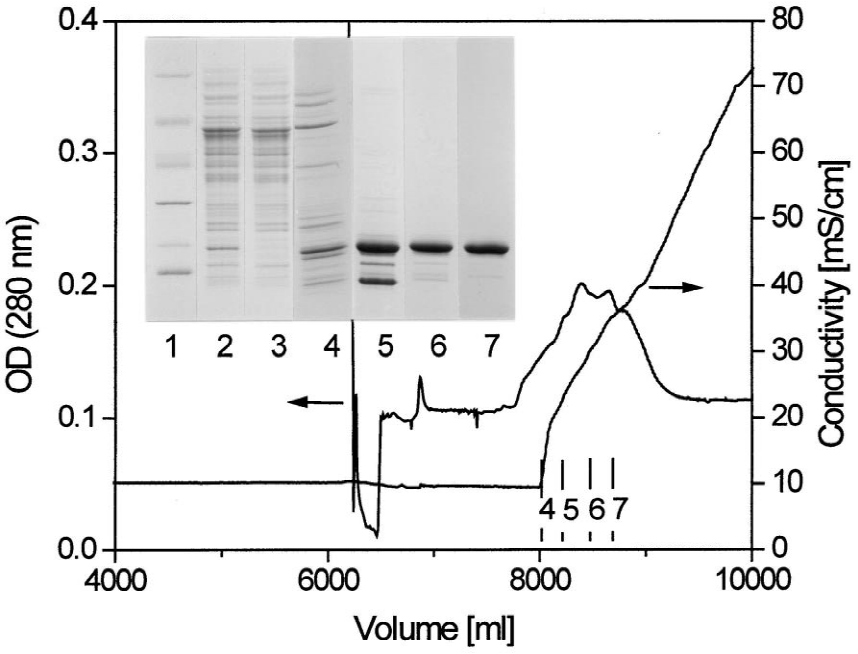

Fig. 5. Separation of 5580 ml crude *E. coli* feedstock on Streamline SP (300 ml) in expanded bed mode at a linear velocity of 150 cm/h in 50 m*M* NaPi + 0.04 *M* NaCl + 1 m*M* EDTA, pH 7, $\kappa = 10$ mS/cm. Inset: SDS–PAGE gels (8–18%) with (1) molecular weight standards ($14 \cdot 10^3$, $20 \cdot 10^3$, $30 \cdot 10^3$, $43 \cdot 10^3$, $67 \cdot 10^3$ and $94 \cdot 10^3$), (2) the feedstock, (3) the breakthrough and fractions 4, 5, 6, 7, as indicated.

(SWISS-PROT data bank, P02341/42), which is almost the same as with rh-bFGF (pI 9.6). This is probably the reason that both proteins were not separated from the cation-exchanger in the salt gradient. The fractions containing rh-bFGF were identified by SDS–PAGE and pooled for further purification by heparin affinity chromatography.

4.4. Heparin affinity chromatography

The CIP stability of affinity chromatographic matrices is an important point to consider, as it allows common cleaning protocols to be applied routinely. With heparin sorbents different experiences were made regarding the stability under normal operation and CIP [37,38]. As heparin is purified from proteoglycans, it displays a heterogenous composition with remaining protein content. Besides the necessity to employ suitable immobilization chemistry, more stable heparin sorbents result when immobilizing only the polysaccharide chain.

Heparin HyperD was chosen as affinity matrix, as it displayed only a minor decrease in capacity under CIP conditions with using up to 0.5 *M* NaOH and lysozyme as model protein in parallel experiments (data not shown). In the present investigation 3 *M* NaCl was found sufficient for column cleaning. No change of the protein binding capacity nor the selectivity was observed.

Batch adsorption isotherms were investigated with purified rh-bFGF to figure out the dependence of thermodynamic constants on ionic strength (Fig. 6). As known from the literature [8], rh-bFGF binds very strongly to heparin. This is confirmed with Fig. 6, from which it is suggested to apply the eluate from the EBA column, whose conductivity corresponds to 0.5 *M* NaCl, directly onto the heparin sorbent, by that circumventing dialysis.

A low but constant UV reading is apparent in the breakthrough of the Heparin HyperD column in Fig. 7. The corresponding substance was concentrated on an anion-exchanger (Q-Sepharose FF), demonstrating the typical adsorption maximum of DNA at 260 nm (data not shown). Also HU protein is found in breakthrough fractions owing to the high ionic strength, which prevent nonspecific binding due to ionic interactions. A small amount of host-derived

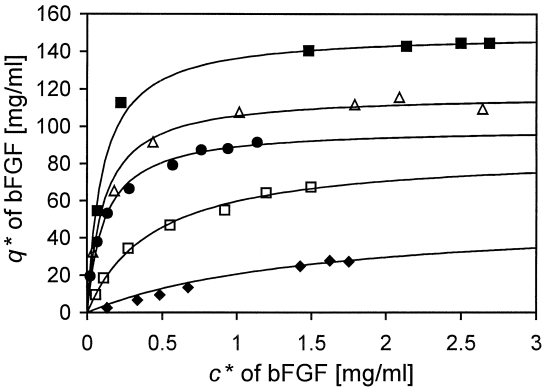

Fig. 6. Batch adsorption isotherms of purified rh-bFGF on Heparin HyperD at different ionic strengths. The solid lines were fitted with the Langmuir equation. ■ = 0 *M* NaCl (κ = 6.27 mS/cm), △ = 0.3 *M* NaCl (κ = 36.2 mS/cm), ● = 0.5 *M* NaCl (κ = 49.9 mS/cm), □ = 0.65 *M* NaCl (κ = 62.4 mS/cm) and ♦ = 1.0 *M* NaCl (κ = 88.2 mS/cm).

proteins eluted in the gradient between 0.5 and 1 *M* NaCl (see inset). At higher salt concentrations the monomer of rh-bFGF elutes as the major peak, followed by the dimer at about 2 *M* NaCl.

Investigating on the influence of flow-rates on peak dispersion, only a minor broadening was observed with increasing flow-rates from 2 to 6 ml/min (data not shown). This indicates that the throughput is not limited by mass transport in the range of recommended flow-rates. A higher flow-rate may have been possible; however, it was restricted by the pressure limit of the glass columns used. Therefore, changing the flow-rate with this affinity sorbent is appropriate to adapt the affinity purification step to a time scale prescribed by process volumes within a purification protocol (i.e. from expanded bed eluates).

In order to achieve an optimal productivity without losing rh-bFGF in breakthrough fractions, different loading volumes and rh-bFGF concentrations were applied (Fig. 7). No breakthrough was observed with applying up to 540 ml, which corresponds to 65% of the maximum column capacity according to batch adsorption isotherms. Therefore, also loading at the high ionic strength allows to utilize most of the static capacity of the heparin sorbent with rh-bFGF. This is an indication for fast reaction kinetics and low mass transfer restrictions.

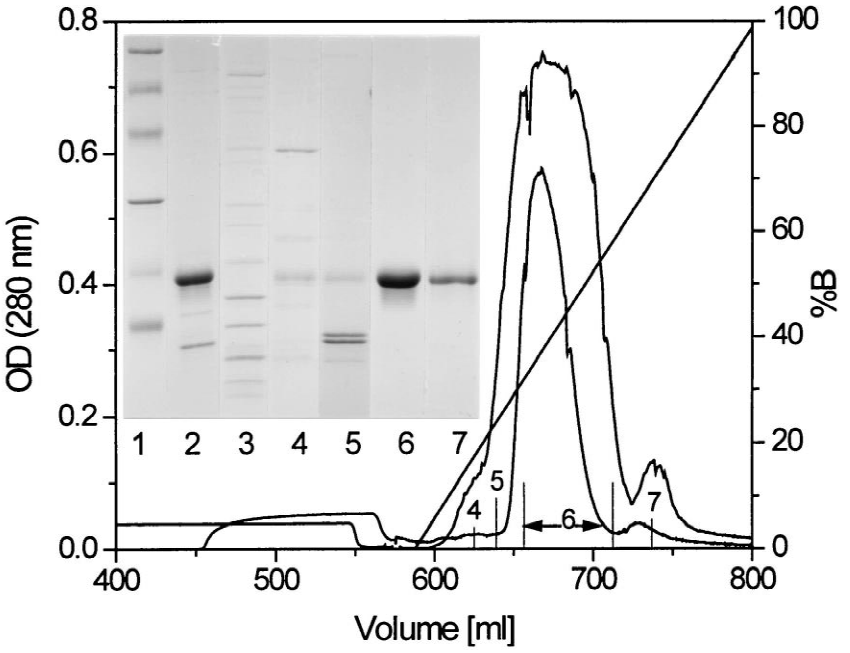

Fig. 7. Separation of expanded bed eluates at two different conditions on Heparin HyperD. Upper curve: a volume of 540 ml was loaded with a flow-rate of 4 ml/min, $\kappa = 20$ mS/cm and c^0(rh-bFGF) = 1.2 mg/ml. Lower curve: 98 ml was loaded with a flow-rate of 3 ml/min, $\kappa = 46.9$ mS/cm and c^0(rh-bFGF) = 2.66 mg/ml. Elution was performed at 2 ml/min with buffer B: 50 m*M* sodium phosphate + 3.0 *M* NaCl + 1 m*M* EDTA, pH 6.3. Inset: SDS–PAGE gels (10–12%) with (1) molecular mass standards ($14 \cdot 10^3$, $20 \cdot 10^3$, $30 \cdot 10^3$, $43 \cdot 10^3$, $67 \cdot 10^3$ and $94 \cdot 10^3$), (2) the loading sample, (3) the breakthrough and fractions 4, 5, 6, 7, as indicated, which correspond to the lower curve.

4.5. Product characterisation

Besides SDS–PAGE gels (see above), matrix assisted laser desorption ionization time of flight (MALDI–TOF) mass spectrometry proved the purity of the affinity-purified rh-bFGF (data not shown). No peaks were detected at a mass to charge ratio m/z of about 9200, corresponding to the HU protein. The main peak at $m/z = 17\,560$ represents the single charged bFGF monomer. At $m/z = 8777$ and 35 098 peaks with lower intensity were found, corresponding to the double charged monomer and the dimer of rh-bFGF, respectively. From this data judging is not possible, whether the dimer was formed due to photochemical reaction or disulfide bridges.

BALB 3T3 cells were used to check the mitogenic activity of purified rh-bFGF before and after lyophilization (Fig. 8). Half-maximal stimulation (ED_{50}) was achieved at 1 to 1.5 ng/ml rh-bFGF with both, which is the same concentration range reported in literature [3]. Higher concentrations cause a lower stimulation of DNA synthesis [39]. Taking into consideration the large fluctuation of the biological test with errors shown as standard deviation in Fig. 8, the mitogenic activity before and after lyophilization is in the same range. Therefore, lyophilization is probably an appropriate method for protein storage.

The endotoxin level decreased during the purification process without special precautions from about 10^6 EU/ml in the cell homogenate to 10^4 EU/ml in the expanded bed elute to a final level of 10 EU/ml at a rh-bFGF concentration of 3 mg/ml. This is due to the strongly negatively charged endotoxin molecules, which is rejected both from cation-exchange and negatively charged heparin ligands and therefore elutes in breakthrough fractions. This is acceptable for clinical application. However, it should be mentioned that endotoxin is masked against the LAL assay by the positively charged rh-bFGF, causing an underestimation of the endotoxin concentration. This can be avoided by digestion of the protein with

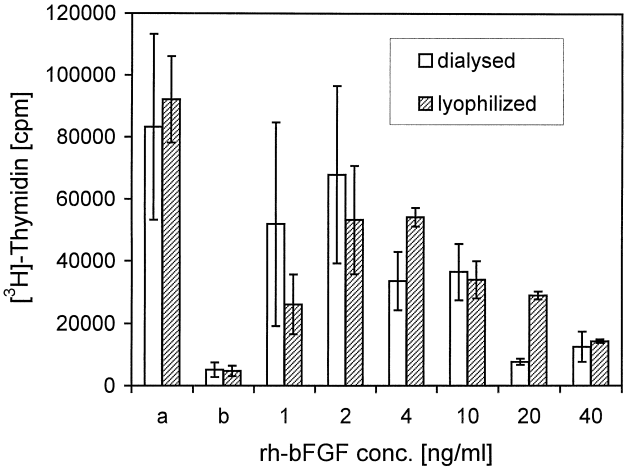

Fig. 8. Stimulation of [^{3}H]-thymidine incorporation into DNA of serum depleted BALB 3T3 cells by purified rh-bFGF prior and after lyophilization. The positive control (a) was stimulated with 10% fetal calf serum and the negative control (b) only with PBS. Error bars indicate the standard deviation from three independent measurements.

proteinase K [40]. Indeed, after protein digestion an increase of the endotoxin level was found. Yet, also the endotoxin level after digestion was still below critical (data not shown).

For a potential use of the rh-bFGF in vivo further problems are to be addressed. So the remaining concentration of DNase is to be followed by ELISA and also leakage of heparin from the affinity column must be scrutinized, as heparin inhibits blood coagulation.

4.6. Process efficiency

Process characteristic data, such as volumes, protein concentrations and recoveries are summarized in Table 3. To compare purification schemes or chromatographic steps with other protocols, the productivity is commonly defined as the throughput per volume of chromatographic media. It has to be kept in mind that such a comparison is only meaningful for fully optimized steps, a criterion that does not apply here.

Assuming the process time of a chromatographic step and the recovery being independent from the scale, comparison of different protocols in terms of overall process time and recovery is possible. In order to compare three protocols developed with time for the purification of rh-bFGF, a relative production rate, R (s^{-1}) is defined as the amount of purified to crude rh-bFGF per time unit. The different purification schemes are outlined in Fig. 9. It should be considered that schemes A and C are early

Table 3
Purification of rh-bFGF from unclarified *E. coli* homogenate

Material	Volume (ml)	Total protein (g)	Conc. (mg/ml)	Total rh-bFGF (g)	Conc. (mg/ml)	Recovery	Purification factor
Crude cell homogenate	5580	57.42	10.29	3.12	0.56	100%	1
Expanded bed eluate	1024	3.03	2.96	2.72	2.66	87%	17
Heparin eluate [a]	585 [56]	2.03 [0.194]	3.46	2.03 [0.194]	3.46	65%	18

[a] Based on an injection of 98 ml (~1/10) of the expanded bed eluate, data given in brackets.

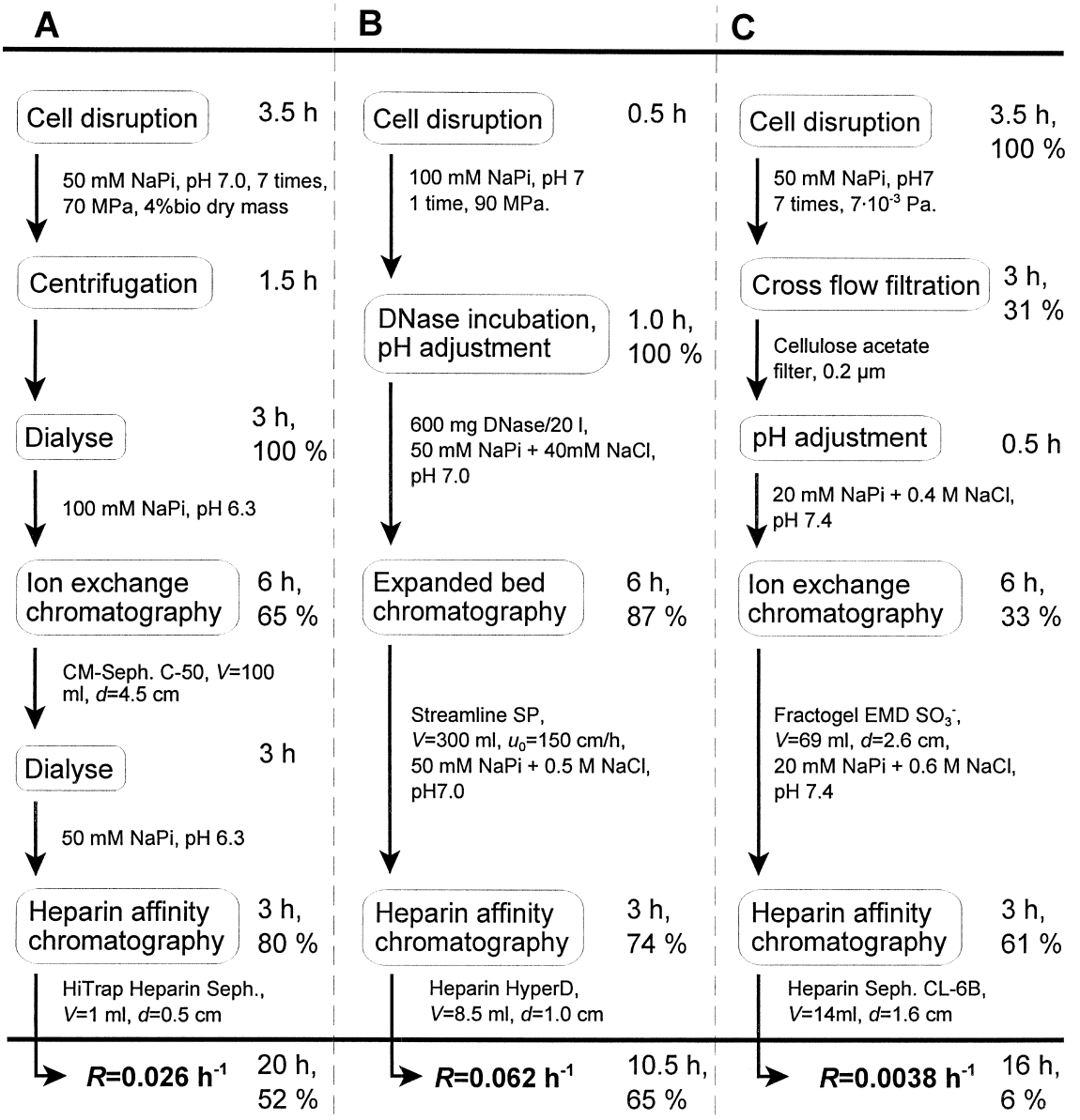

Fig. 9. Process effectivity of three different schemes for rh-bFGF. Scheme A is adapted from Seeger et al. [41], C from Rantze [42] and B is this investigation. The process times of chromatographic purification steps were set equal to make it comparable in relation to different scales.

steps in the development of rh-bFGF production with a different intention than to optimize the downstream process. Owing to a circumvention of clarification and dialysis, the process utilizing expanded bed adsorption is quickest with an overall process time of 11 h. Furthermore, the straightforward operation after cell disruption reduces product losses through protease activity and shear stress, as may occur during filtration, and increases the product recovery. Consequently, the relative production rate is 2.3, which is 16 times higher than in schemes A and C, respectively.

5. Conclusion

The combination of a strong cation-exchange sorbent in an expanded bed mode and a heparin affinity chromatographic step results in a very efficient protocol for purification of rh-bFGF produced with high cell density cultivation in *E. coli*. The expanded bed mode links clarification, microfiltration and concentration of rh-bFGF in an integrated product capture step, resulting in an increased product recovery compared with conventional procedures. Knowledge of the binding capacities and association constants at different ionic strengths allows direct application of cation-exchange eluates onto the heparin matrix without prior dialysis. The rigid matrix of Heparin HyperD, which did not show any gel compression at recommended flow-rates, can be employed over a wide range of flow-rates without loss of separation performance. The overall process is suitable for scale up and resulted in a product with high mitogenic activity. Also, a high recovery of 65% based on the rh-bFGF concentration in the crude homogenate could be realized. Furthermore, the process significantly reduced the endotoxin level below toxic concentrations.

6. Symbols

c^*	equilibrium concentration of rh-bFGF (mg ml^{-1})
c^0	initial liquid phase concentration of rh-bFGF (mg ml^{-1})
d_p	particle diameter (m)
D_{eff}	effective pore diffusion coefficient of adsorbate (m^2 s^{-1})
g	acceleration of gravity (m s^{-2})
h	bed height (cm)
h_0	sedimented bed height
k_f	liquid film mass transfer coefficient (m s^{-1})
K	consistancy index (power law)
K_D	equilibrium constant for the Langmuir isotherm (mg/ml)
m	flow index (power law)
N	theoretical plate number
q^*	binding capacity of rh-bFGF at the sorbent (mg/ml)
q_m	maximum binding capacity of rh-bFGF (mg/ml) from Langmuir equation
R	relative production rate (s^{-1})
r_p	particle radius (m)
u_0	superficial velocity (m s^{-1})
u_t	terminal settling velocity (m s^{-1})

Greek letters

ε	void fraction of expanded bed
ε_0	void fraction of sedimented bed
ε_p	particle porosity
$\dot{\gamma}$	shear rate (s^{-1})
κ	conductivity (mS/cm)
η	fluid viscosity (mPa s)
ρ_l	liquid phase density (g/ml)
ρ_s	composite particle density (g/ml)
τ	fluid shear stress (mPa)

Abbreviations

CIP	cleaning in place
cpm	counts per minute
EBA	expanded bed adsorption
EU	Endotoxin units, 1 EU/ml = 0.1 ng/ml
HU	Histone like protein
OD	optical density at 280 nm
PBS	phosphate-buffered saline
rpm	revolutions per minute

Acknowledgements

We gratefully acknowledge A. Walter for technical assistance, M. Schmidt for high cell density cultivation of *E. coli*, R. Hartmann for installing the expanded bed equipment, N. Papamichael for writing the programme DAMOCLeS, R. Getzlaff for N-terminal sequence analysis, T. Behn for assaying the mitogenic activity, D. Meschkat for endotoxin determination, and S. Wassmann for the MALDI–TOF measurement.

References

[1] W.H. Burgess, T. Maciag, Annu. Rev. Biochem. 58 (1989) 575.

[2] A. Baird, P. Böhlen, in: M.B. Sporn, A.B. Roberts (Eds.), Peptide Growths Factors and Their Receptors I, Springer Verlag, Berlin, Germany, 1990, p. 369.
[3] C.H. Squires, J. Childs, S.P. Eisenberg, P.J. Polverini, A. Sommer, J. Biol. Chem. 263 (1988) 16297.
[4] Y. Ke, M.C. Wilkinson, D.G. Fernig, J.A. Smith, P.S. Rudland, R. Barraclough, Biochim. Biophys. Acta 1131 (1992) 307.
[5] A. Bikfalvi, S. Klein, G. Pintucci, D.B. Rifkin, Endocrine Rev. 18 (1997) 26.
[6] M. Klagbrun, J. Folkman, M.B. Sporn, A.B. Roberts (Eds.), Peptide Growths Factors and Their Receptors, II, Springer Verlag, Berlin, Germany, 1990, p. 549.
[7] Scios Nova, Mountain View, CA, 1999, USA.
[8] R.R. Lobb, J.W. Harper, J.W. Fett, Anal. Biochem. 154 (1986) 1.
[9] Y. Shing, Methods Enzymol. 198 (1991) 91.
[10] C. George-Nascimento, J. Fedor, in: E.L.V. Harris, S. Angal (Eds.), Protein Purification Applications, Oxford University Press, Oxford, Great Britain, 1989, p. 128.
[11] H.A. Chase, Trends Biotechnol. 12 (1994) 296.
[12] J. Thömmes, Adv. Biochem. Eng. 58 (1997) 185.
[13] R. Hjorth, Trends Biotechnol. 15 (1997) 230.
[14] R. Hjorth, S. Kämpe, M. Carlsson, Bioseparation 5 (1995) 217.
[15] G.M.S. Finette, Q.-M. Mao, M.T.W. Hearn, Biotechnol. Bioeng. 58 (1998) 35.
[16] C. Zurek, E. Kubis, P. Keup, D. Hörlein, J. Beunink, J. Thömmes, M.-R. Kula, C.P. Hollenberg, G. Gellissen, Process Biochem. 31 (1996) 679.
[17] F. Raymond, D. Rolland, M. Gauthier, M. Jolivet, J. Chromatogr. B 706 (1998) 113.
[18] G. Maurizi, V. di Cioccio, G. Macchia, P. Bossù, C. Bizzarri, U. Visconti, D. Boraschi, A. Tagliabue, P. Ruggiero, Protein Expression Purification 9 (1997) 219.
[19] H.J. Johansson, C. Jägersten, J. Shiloach, J. Biotechnol. 48 (1996) 9.
[20] B.C. Batt, V.M. Yabannavar, V. Singh, Bioseparation 5 (1995) 41.
[21] J. Thömmes, A. Bader, M. Halfar, A. Karau, M.-K. Kula, J. Chromatogr. A 752 (1996) 111.
[22] A.-K. Barnfield Frej, H.J. Johansson, S. Johansson, P. Leijon, Bioprocess Eng. 16 (1997) 57.
[23] M. Leonard, J. Chromatogr. B 699 (1997) 3.
[24] E. Boschetti, J.L. Coffman, in: G. Subramanian (Ed.), Bioseparation and Bioprocessing, Wiley-VCH, Weinheim, Germany, 1998, p. 157.
[25] I. Machač, P. Mikulášek, I. Ulbrichová, Chem. Eng. Sci. 48 (1993) 2109.
[26] J.F. Richardson, W.N. Zaki, Chem. Eng. Sci. 3 (1954) 65.
[27] R. di Felice, Chem. Eng. Sci. 50 (1995) 1213.
[28] A. Seeger, B. Schneppe, J.E.G. McCarthy, W.-D. Deckwer, U. Rinas, Enzyme Microb. Technol. 17 (1995) 947.
[29] G. Garke, I. Radtschenko, F.B. Anspach, J. Chromatogr. A 857 (1999) 137.
[30] O.H. Lowry, N.J. Rosenbrough, A.L. Farr, R.J. Randall, J. Biol. Chem. 193 (1951) 265.
[31] U.K. Laemmli, Nature 227 (1970) 680.
[32] H.A. Weich, N. Iberg, M. Klagsbrun, J. Folkman, Growth Factors 2 (1990) 313.
[33] A.-K. Barnfield Frej, R. Hjorth, Å. Hammarström, Biotechnol. Bioeng. 44 (1994) 922.
[34] A.I. Liapis, D.W.T. Rippin, Chem. Eng. Sci. 32 (1977) 619.
[35] G. Garke, R. Hartmann, N. Papamichael, W.-D. Deckwer, F.B. Anspach, Sep. Sci. Technol. 1999, in press.
[36] M.E. Young, P.A. Carroad, R.L. Bell, Biotechnol. Bioeng. 22 (1980) 947.
[37] H. Sasaki, A. Hayashi, H. Kitagaki-Ogawa, I. Matsumoto, N. Seno, J. Chromatogr. 400 (1987) 123.
[38] F.B. Anspach, H.S. Spille, U. Rinas, J. Chromatogr. A 711 (1995) 129.
[39] P.V. Milev, O.I. Georgiev, P.O. Tzaroretchki, A.A. Hadjiolov, J. Biotechnol. 22 (1992) 299.
[40] D. Petsch, W.-D. Deckwer, F.B. Anspach, Anal. Biochem. 259 (1998) 42.
[41] A. Seeger, U. Rinas, J. Chromatogr. A 746 (1996) 17.
[42] E. Rantze, Diploma Thesis, Technical University of Hannover, Germany, 1996.